A R C H I V E O F M E C H A N I C A L E N G I N E E R I N G

VOL. LXV 2018 Number 3

DOI: 10.24425/124487

Key words: erosion, CFD, multi-phase flow, pressure drop

VIKAS KANNOJIYA[1], *M.B. DARSHAN*[1], *YOGENDER PAL CHANDRA*[2]

NUMERICAL ANALYSIS OF EROSION WEAR AND PRESSURE DROP FOR TURBULENT MULTIPHASE SLURRY FLOW OF BOTTOM ASH-WATER IN SLURRY PIPE

The disposal of ash in a thermal plant through the slurry pipe is subjected to some erosion wear due to the abrasive characteristics of the slurry. A simulation study of particle-liquid erosion of mild steel pipe wall based on CFD-FLUENT that considers the solid-liquid, solid-solid and solid-wall interaction is presented in this work. The multi-phase Euler-Lagrange model with standard k-ϵ turbulence modeling is adopted to predict the particulate erosion wear caused by the flow of bottom ash-water suspension. Erosion rate for different particle size and concentration is evaluated at variable flow rate. It is observed that the pressure drop and erosion rate share direct relationships with flow velocity, particle size and concentration. The flow velocity is found to be the most influencing parameter. A model capable of predicting the erosion wear at variable operating conditions is presented. The simulation findings show good agreement with the published findings.

Nomenclature

D	Diameter, m
P	Pressure, N m^{-2}
Re	Reynolds number
Re$_p$	Particle Reynolds number
d_p	Particle diameter, m
m_p	Particle mass, kg

[1] *Department of Mechanical and Industrial Engineering, Indian Institute of Technology, Roorkee, India; Emails: vikas.passion.singh@gmail.com; mb.darshan2373@gmail.com*

[2] *Faculty of Mechanical Engineering, Department of Environmental Engineering, Czech Technical University, Prague, Czech Republic; Email: yogender027mae@gmail.com*

u_p	Particle velocity, m s^{-1}
T	Time, s
K	Turbulence kinetic energy, m^{2}s^{-2}
v	Fluid velocity, m s^{-1}
g	Gravitational acceleration, m s^{-2}
V_r	Particle relative velocity, m s^{-1}
ρ_f	Fluid density, kg m^{-3}
ρ_p	Particle density, kg m^{-3}
μ_{eff}	Effective viscosity for fluid phase, Pa s
ϵ	Dissipation rate of fluid turbulence, m^{2}s^{-3}
C_d	Drag coefficient

1. Introduction

Ash transport system, that employs water or air to convey solid ash particles through the slurry pipeline, is a crucial element of many thermal power plants. Straight pipes are the most common part of a pipeline unit [1]. The total ash produced in a thermal power station comprises almost 80% of fly ash and 20% bottom ash in it [2]. The bottom is conveyed in the form of a multiphase slurry of water and solid particles of bottom ash. The solid particles deviate from the fluid stream and strike on the surface of the pipe wall that exhibits wear (erosion) in the form of material removal. The material loss may lead to severe damage to the pipe and also results in pipe failure. Due to this serious concern, several studies have been reported that focus on the analysis of erosion wear under various influencing parameters and their relationship with erosion rate [3, 4]. The dependence of erosion wear on a large number of parameters makes it very difficult to observe this phenomenon. The parameters like flow, target material and solid properties have a significant influence on the erosion wear characteristics [5–7].

Many investigators conducted both experimental and computational study to investigate wear in pipe line [7–9]. Computational fluid dynamics (CFD) emerges to be an effective tool to analyze particulate erosion. Particulate wear in the straight pipeline has been investigated by several researchers [8–17].

Authors of [16] conducted an experimental analysis of wear rates in a bottom ash disposal pipeline. The study was conducted on a slurry pipe loop for the flow of water-bottom ash slurry. The influence of various operating parameters on the wear rate of the pipeline was investigated. The possibility of wear reduction by adding fly-ash in the slurry was also discussed. In [17] a simulation study of solid-liquid flow in the horizontal straight pipe is reported. An ANSYS-CFX based 3-D hydrodynamic model was used for the simulation investigations. Authors examined the effect of operating parameters like solid concentration, solid size, mixture velocity and pipe diameter on the frictional pressure loss. The simulation findings were also compared with the published experimental

data and found to be in excellent agreement with them. Some researchers examined the effect of solid size on the pipeline friction due to the flow of Newtonian slurry [18].

In [11] authors have analyzed the erosion and particle distribution on straight and curved pipe geometry under different flow condition of Newtonian and non-Newtonian slurries. The flow solution has been achieved by employing Euler-Euler approach in the CFD code FLUENT. A comprehensive study on flow distribution was reported in their study. A comprehensive study of erosion wear on typical components of oil pressure pipeline was performed in [19]. Authors study was focused on the differently angled pipe bends and sudden expansion pipes. They reported high erosion wear on bends, whereas sudden expansion pipes experienced less wear. Authors of [20] investigated erosion wear rate on 90° bend using Discrete phase model (DPM) for the flow of water and copper particles. They examined the influence of velocity and particles size on pipe erosion wear at different solid concentrations. In [12] a probability model to calculate the erosion caused by the solid particles in a straight pipe was developed. The effect of particle size (50–400 μm), pipe diameter (50.5 to 203.2 mm) and flow velocity (3.048–15.240 m/s) on erosion rate was investigated. The model was then verified with the results obtained by experiments and CFD simulations. The influence of pipe diameter was found to be having an inverse relation with the erosion rate. Penetration rate was increased up to 6.4 times at the velocity shifted from 3.048 m/s to 6.096 m/s.

A literature survey shows that the erosion wear behavior in the conveying pipeline can be effectively analyzed by CFD tools. Many researchers are considering erosion in pipe bends but the wear in the straight pipe is significant enough and cannot be ignored. In recent times, several researches have been focused mainly on the flow simulation of sand or fly ash slurry, on the other hand, the studies on the complex flow of bottom ash slurry are quite limited. Therefore, in the study, the simulation of erosion wear for the bottom ash-water slurry was performed by using commercial Ansys code Fluent with Discrete Phase Modeling (DPM). The wear investigation was performed on a 0.050 m diameter and 2 m long mild steel straight horizontal pipe. The flow variations were solved by adopting standard k-ϵ turbulence model while enhanced wall treatment was applied to accurately observe the flow phenomenon near the pipe wall. The simulation study of wear was performed under a different influencing operating condition, such as flow velocity (2–8 m/s), particle diameter (50–350 μm) and solid concentration (2–10%).

1.1. Thermal Power Ash Disposal System

Energy generation in thermal power plants by burning the fed coal generates a large amount of ash as a side product. The total generated ash comprised of approximately 20% of bottom ash and 80% of fly ash. The slurry pipelines are

extensively used to transport the coal ash to the disposal unit. (Fig. 1) illustrates a typical layout of ash distribution unit in a thermal power plant.

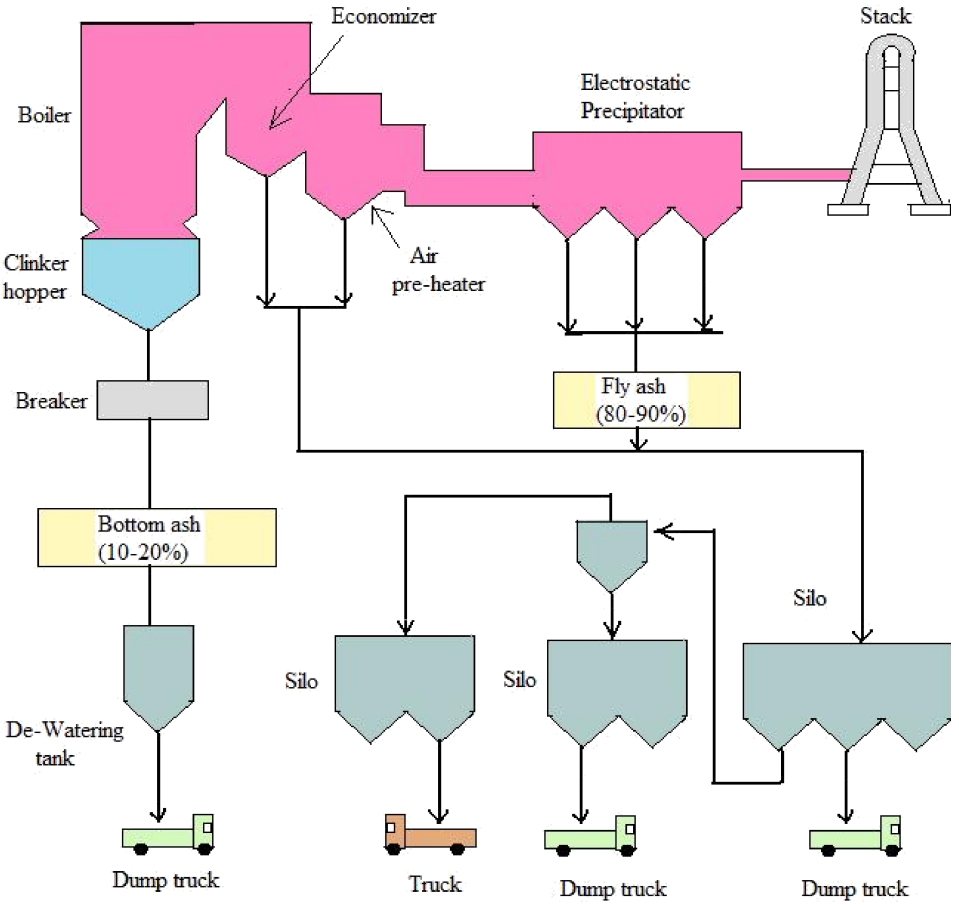

Fig. 1. Layout of ash distribution unit in thermal power plant

1.2. Bottom ash transport system

The fine ash particles that rise along with the flue gas are known as fly ash, collected through electrostatic precipitator and sent to the utilization unit through the fly ash handling unit. On the other hand, the clinkers formed by the residue of un-combustible impurities present in the coal are termed as bottom ash. These clinkers are then crushed into a smaller size, mixed with water to form the slurry and then conveyed to the utilization unit through bottom ash handling unit. A layout of bottom ash handling system of a thermal power plant is shown in Fig. 2.

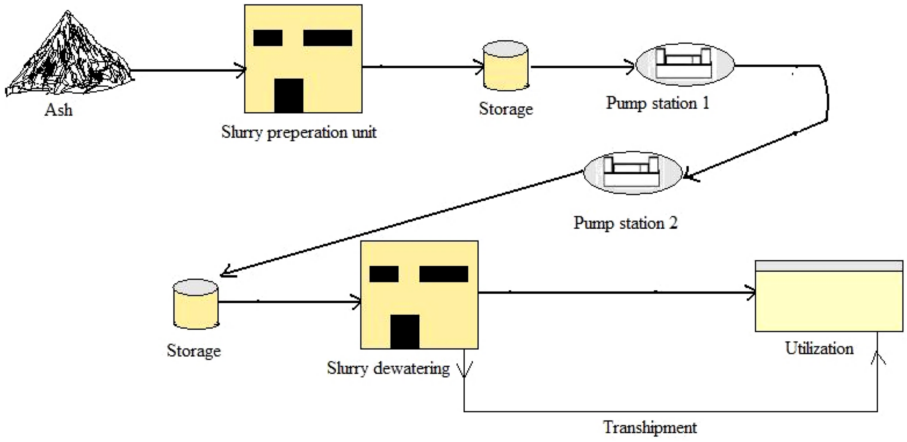

Fig. 2. Bottom ash handling system

2. Numerical modeling

The numerical modeling was divided into three important components as Flow modeling, discrete phase modeling, and erosion modeling. A Euler–Lagrange based discrete phase model was implemented in this work using Ansys-CFD. Each model will be discussed in detail.

2.1. Flow modeling

The following governing equations were implemented to solve the multiphase flow of solid–liquid.

Continuity equation:

$$\frac{\partial \rho_f}{\partial t} + \nabla \cdot \left(\rho_f v_f\right) = 0. \tag{1}$$

Momentum equation:

$$\frac{\partial \rho_f v_f}{\partial t} + \nabla \cdot \left(\rho_f v_f v_f\right) = -\nabla + \nabla \cdot \left[\mu \left(\nabla v_f + \nabla v_f^{\mathrm{T}}\right)\right] + \rho_f g. \tag{2}$$

The turbulent fluid flow in the pipeline is solved by applying standard k-ϵ model. The governing equations for this model are:

Kinetic energy transport equation:

$$\frac{\partial \rho_f k}{\partial t} + \nabla \cdot \left(\rho_f v_f k\right) = \nabla \cdot \left[\left(\mu + \frac{\mu_t}{\sigma_k}\right) \nabla k\right] + G_k \rho_f \epsilon. \tag{3}$$

Dissipation equation for turbulent kinetic energy transport:

$$\frac{\partial \rho_f \epsilon}{\partial t} + \nabla \cdot \left(\rho_f v_f \epsilon\right) = \nabla \cdot \left[\left(\mu + \frac{\mu_t}{\sigma_\epsilon}\right) \nabla \epsilon\right] + \frac{\epsilon}{k}(C_{\epsilon 1} G_k - \rho \epsilon C_{\epsilon 2}). \tag{4}$$

Table 1.

Coefficient's default value for k-ϵ standard model

$C_{\epsilon 1}$	$C_{\epsilon 2}$	σ_k	σ_ϵ
1.44	1.92	1	1.3

2.2. Discrete phase modeling

The fluid phase was treated as a continuous phase and its solution was obtained by using Euler formulation based on Navier–Stokes equation while the particle motion was modeled by using discrete phase algorithms. The solution of discrete phase was based on Lagrange technique. The motion of the solid particle is mainly influenced by drag and gravity force and can be predicted by integrating the force balance equation which equates the inertia of the particle to the force acting on the particle, as described in equation (5) (for x coordinate and in Cartesian coordinate). Some of the assumptions for modeling discrete phase are summarized in Table 2.

$$\frac{\mathrm{d}\, v_f}{\mathrm{d}\, t} = F_D(v_f - v_p) + \frac{g_x(\rho_p - \rho_f)}{\rho_f} + F_x\,. \tag{5}$$

Here, F_x is the additional force in the force balance of particles representing the virtual mass force needed to accelerate the fluid adjacent to the accelerating particle. The dimension of F_x are ms^{-2}, quite similar to the unit of acceleration, $F_D(v_f - v_p)$ is the drag force per particle.

Table 2.

Assumptions to model discrete phase

Solid particle	Density ($\mathrm{kg/m}^3$)	Tracking parameter: maximum number of steps	Reflection coefficient at wall		Particle shape
			Normal	Tangent	
Bottom ash	2200	10000	Polynomial	Polynomial	Spherical

The influencing drag force applicable on the particles is given by:

$$F_D = \frac{18\mu}{\rho_p d_p^2} + \frac{C_{D0} R_e}{24}\,, \tag{6}$$

where C_{D0} is the coefficient of drag and can be expressed as:

$$C_{D0} = a_1 + \frac{a_2}{\mathrm{Re}} + \frac{a_3}{\mathrm{Re}}\,, \tag{7}$$

a_1, a_2 and a_3 are constants applicable for smooth particles provided in [21] for a different Reynaud number; Re_p is the particle's Reynolds number and is written as:

$$\mathrm{Re}_p = \frac{(\rho_f d_p |v_p - v_f|)}{\mu}\,. \tag{8}$$

For "reflect" boundary condition, the energy loss of the particles after its collision with the wall can be accounted by providing some reflection coefficient in the simulation study. Fig. 3 represents the collision of a ash particle with the wall. The two components of the reflection coefficient are described below:

(a) normal component: $e_n = \dfrac{v_{2n}}{v_{1n}}$,

(b) tangential component: $e_n = \dfrac{v_{2t}}{v_{1t}}$.

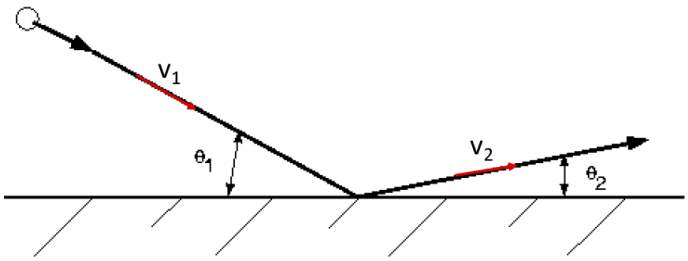

Fig. 3. Particle reflection at wall

2.3. Erosion modeling

The erosion wear rate due to the impingement of ash particles on the pipe wall was monitored by implementing discrete phase model in FLUENT and could be expressed as [22]:

$$R_{erosion}(E) = \sum_{p=1}^{Nparticles} \left(\frac{(\dot{m}_p C(d_p)) f(a) v_p^{b(v)}}{A_f} \right), \tag{9}$$

where E is the Erosion rate caused by solid particles at the pipeline wall. The particle flow rate and velocity is represented by $\dot{m}_p$ and v_p, respectively. The term $f(a)$, $b(v)$ and $C(d_p)$ denotes the function of impact angle, function of particle relative velocity and the function of particle diameter, respectively. A_f represents the cell face area along the wall. The default values of C, f and b are set to $1.89e^{-09}$, 1 and 0, respectively.

3. Computational analysis

3.1. Computational Domain and Mesh

In our case, erosion investigation was performed on a 0.050 m diameter mild steel horizontal pipe. The length of the pipe was 20 times the diameter, i.e., 1 m which was enough to maintain fully developed flow. Fig. 4 represents the flow domain whereas Table 3 shows the details of the flowing domain.

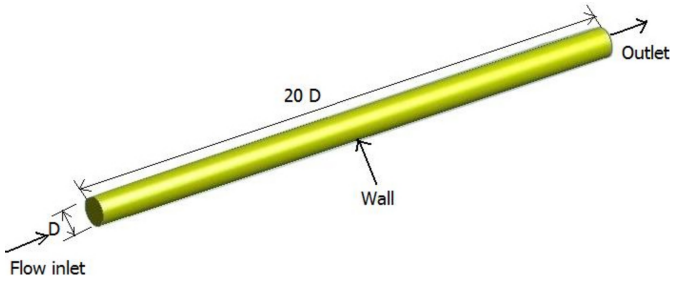

Fig. 4. Horizontal straight slurry pipe

Table 3.

Geometry details

Domain	Detail
Diameter	0.050 m
Position	Horizontal
Length	1 m
Material	Mild steel
Density	7850 kg/m^3

To analyze flow phenomenon precisely at each section of the pipe, the flow domain was divided into smaller tetrahedral elements. As per the grid sensitivity analysis, the flow domain was discretized into 547754 tetrahedral cells. Fig. 5 illustrates the meshing on the pipeline.

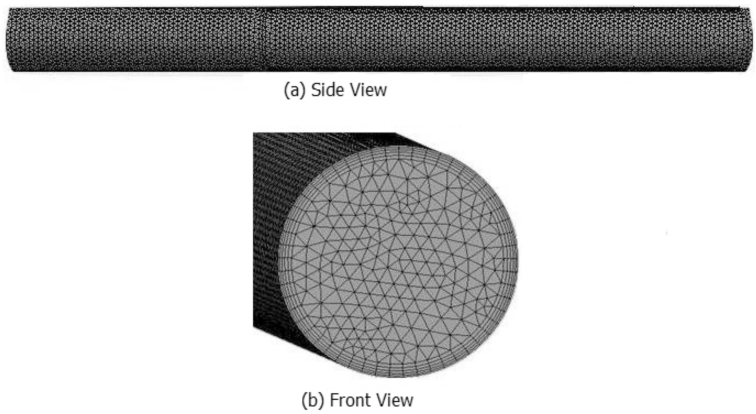

Fig. 5. Meshing on pipeline

3.2. Slurry flow properties

In this work, a simulation study was performed to study the erosion wear of a straight mild steel pipe due to the flow of bottom ash and water multiphase slurry. The size of the bottom ash particles was selected so as to cover all the available

sizes of bottom ash (50–350 μm) in industries [23]. Water is the primary fluid phase, having a density of 1000 kg/m^3. The multiphase property is discussed in detail Table 4.

Table 4.

Property of multiphase flow

Properties	Fluid	Solid
Type	Water	Bottom ash
Density (kg/m^3)	1000	2200
Velocity (m/s)	2–10	2–10
Concentration	–	2–10% (by weight)
Particle size	–	50–350 μm

3.3. Boundary conditions

Boundary conditions for simulating the multiphase flow through the pipe, such as fluid velocity, operating pressure, and density, were required to solve the flow variations. A brief description of the boundary condition is listed in Table 5. The flow variations were solved by adopting standard k-ϵ model, while enhanced wall treatment was applied to accurately observe the flow phenomenon near the pipe wall.

Table 5.

Boundary conditions and model parameters

Modeling parameters	Fluid phase	Discrete phase
Equations of solver	Navier–Stokes	Discrete phase modelling
Flow turbulence model	Standard k-ϵ	
Wall treatment	Standard wall function	
Discrete phase conditions		Reflect
Velocity at inlet	2 m/s	2 m/s
Outlet pressure	Ambient	

The pipe inlet was provided with the constant flow of water having an initial velocity of 2 m/s which was varied from 2 to 8 m/s for further simulations. The pipe outlet was subjected to gauge pressure of 0 bar, while the no-slip condition was adopted for the wall. The interaction of the particle and wall was observed by implementing the stochastic tracking model. This model considers the effect of mean as well as instantaneous turbulent velocity fluctuations on the particle i.e. $U = \bar{u} + u'$. The dispersion of the particles can be obtained by integarating the trajectory equation for the individual particles.

First order upwind was employed for the discretization of all terms. The velocity and diameter functions mentioned in equation 9 were selected as constant with the values of 2.6 and $1.8 \cdot 10^{-9}$, respectively. The convergence limit was set to 10^{-5}.

3.4. Validation

In this section, the present erosion model was examined by comparing with the published findings [12]. They develop a model to investigate particulate erosion wear in a straight pipe. They implemented standard k-ϵ model in CFD code FLUENT to simulate the flow. The wear analysis was performed by varying particle size from 50 to 400 μm at different velocity ranging from 3.048 to 15.20 m/s. The model was then verified with experimental findings. Their results showed that the increase in particle size causes more erosion but up to a certain extent; after that, a limited increment was observed. We have validated some cases of those published in [12] (velocity and particle size variation) by adopting the same boundary condition and material properties. It was observed that the present simulation shows the maximum variation of 8.32 and 9.48% for the velocity and particle size variation cases as represented in Fig. 6a and 6b.

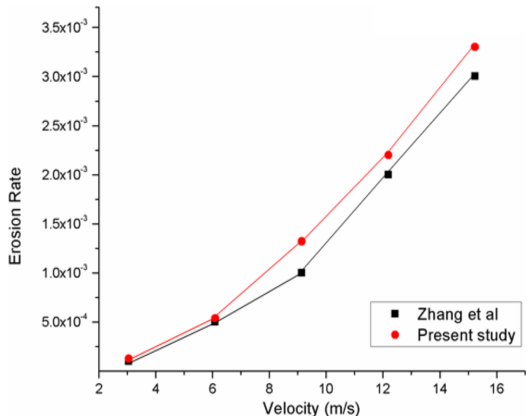

(a)

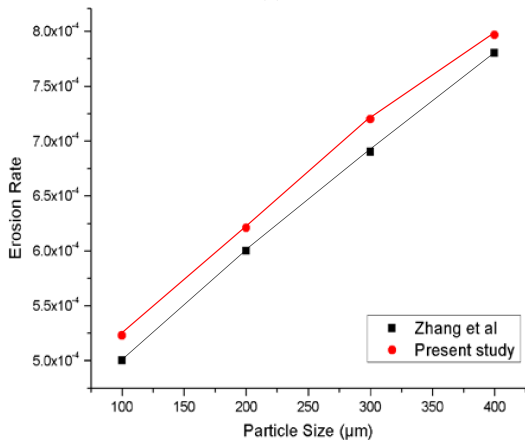

(b)

Fig. 6. Zhang et al. erosion data [12] versus present work at a different: (a) velocity, (b) particle size

4. Results and discussion

In this work, turbulent fluid flow through a horizontal straight slurry pipeline was investigated. The pipe was made of mild steel having 0.05 m diameter and 1 m length. The fluid was water consisted of suspensions of bottom ash particles. The operating conditions and parameters are briefly discussed in Table 6.

Table 6.

Test conditions and parameters

S. No.	Flow velocity (m/s)	Solid diameter (μm)	Solid conc. (by wt.)
1	2	50–350	10%
2	4	50–350	10%
3	6	50–350	10%
4	2–8	200	10%
5	2	50	2–10%
6	4	50	2–10%
7	6	50	2–10%

4.1. Particle size effect

Investigations were carried out to observe the influencing characteristics of the bottom ash particle size on the erosion rate and for the same, the particle size was varied in the span of 50–350 μm at three different velocities as 2, 4 and 6 m/s. The concentration of bottom ash particles in the slurry was kept as 10% by weight. Fig. 7 suggests the influence of the particle diameter on the erosion rate. It can be observed from the figure that the erosion rate gets enhanced with the increase in

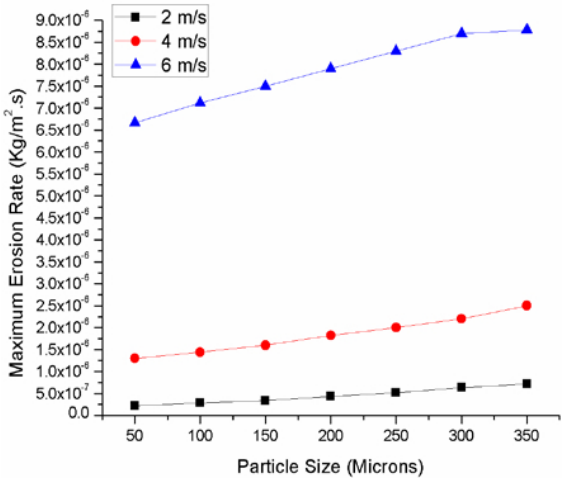

Fig. 7. Influence of particle size on maximum erosion rate

particle size. An enhancement of about 34% in maximum erosion rate is noticed when the particle size increases from 50 to 300 μm. It is also observed that the percentage increment in erosion was greater when the particle size was increased from 50 to 250 μm, whereas, when exceeding 250 μm, the percentage increment in erosion rate was comparatively lower as particle–particle interactions became more significant. Higher particles possess high inertia, thus get deviated from the main flow stream and collide with the wall. The obtained results are in agreements with the results of [8].

4.2. Velocity effect

Flow velocity influences erosion wear in an exponential manner. Fig. 8 illustrates the variation occurring in the magnitude of erosion rate with the change in the flow velocity. It can be noted that the erosion rate magnitude rises significantly with the velocity. In the figure, a considerable difference between the erosion peaks is observed with the change in velocity. An enhancement of approximately 4.1 times in the magnitude of maximum erosion rate was noticed when the flow velocity increased from 2 m/s to 6 m/s. High velocity provides an excess impact force to the ash particles and thus severe collision occurs between them and the pipe wall. A similar kind of increasing trend of erosion rate was also observed by other researches [24].

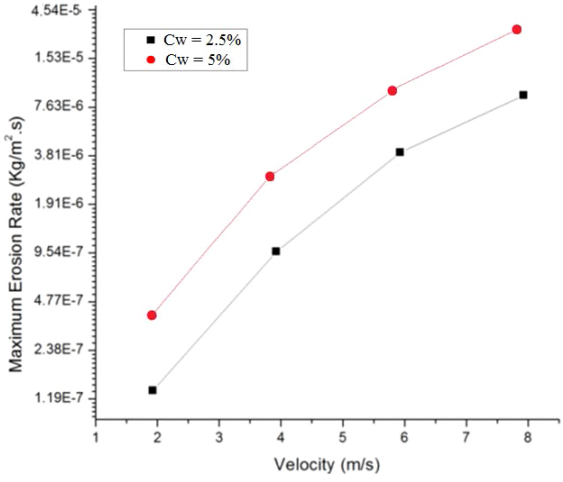

Fig. 8. Influence of flow velocity on maximum erosion rate

The insight into erosion wear due to solid particle impingement on the slurry pipeline can be better visualized by the erosion rate contours, as shown in Fig. 9. The damage of slurry pipe line due to particle impingement is mainly observed near the center to the exit section of the pipeline.

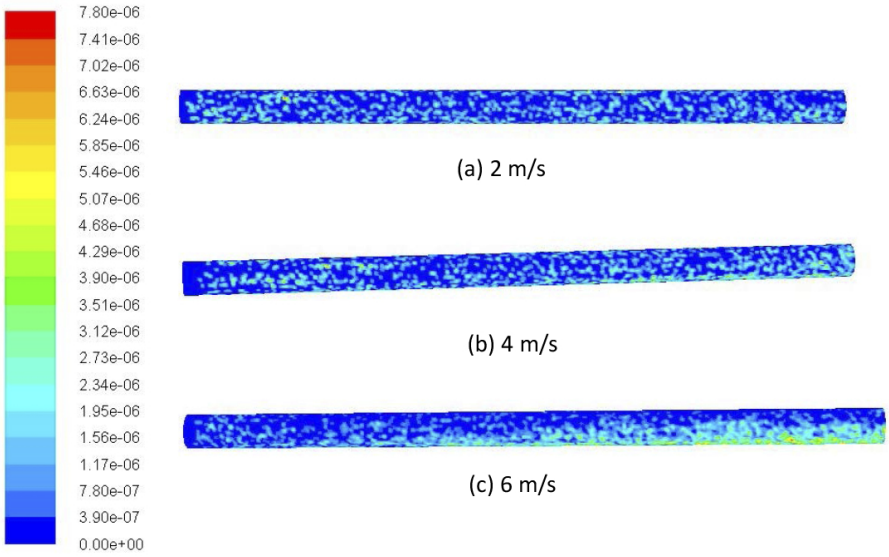

Fig. 9. Contours of erosion rate on the pipe wall for 200 μm sized particles at 10% concentration

The contours of solid concentration at the pipe outlet are plotted at different sections of the pipeline at 4 m/s velocity to observe the dynamics of two-phase slurry flow, as shown in Fig. 10. It was found that, at the mid-length of the pipe, the erodent inertia dominates over the flowing stream and thus higher particle settling is noticed in that regions, which exhibits further increase in the direction of pipe length.

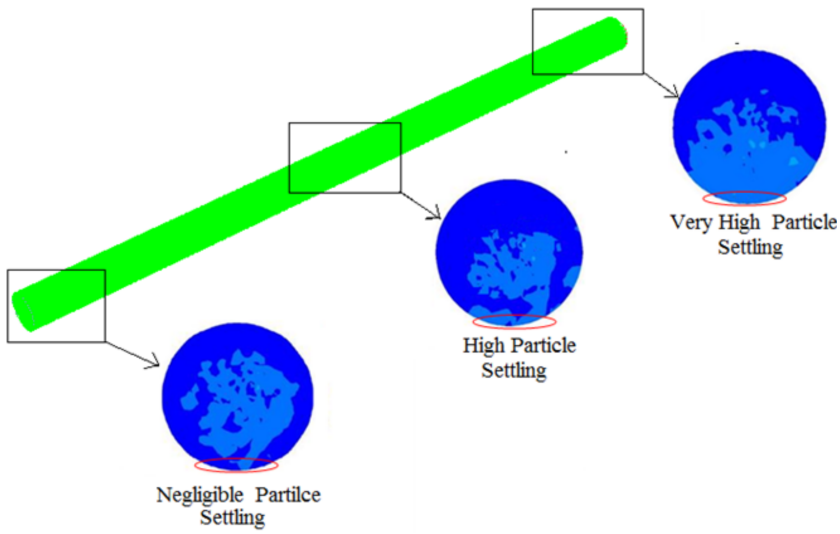

Fig. 10. Discrete phase concentration at different sections of the pipeline for 200 μm size particle

4.3. Erosion rate distribution

Fig. 11 illustrates the erosion rate distribution along the pipe length at 2 m/s velocity for different particle size. From the figure, it is clear that the location of erosion rate is mainly focused from the center to the exit of the slurry pipeline. Moreover, higher wear rate is noticed for bigger sized particles. A region of the significantly less erosion is also observed near the inlet section of the pipeline.

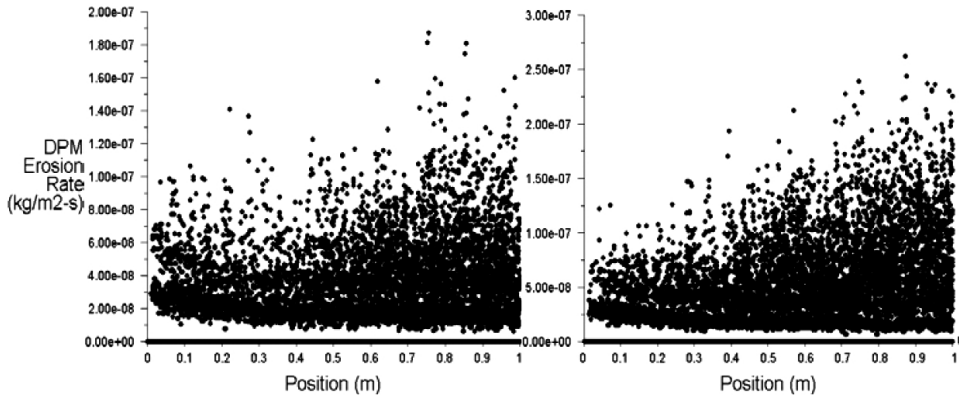

(a) 100 μm (b) 200 μm

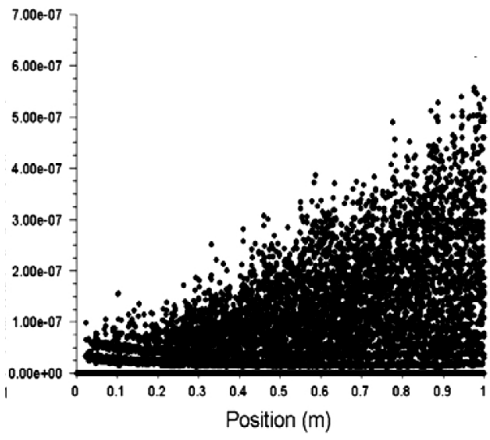

(c) 300 μm

Fig. 11. Erosion rate distribution at pipe wall for different size solid particles

The influence of slurry velocity on the flow turbulence (in percentage) inside the pipe can be observed from the turbulence contours shown in Fig. 12. The slurry flow velocity drastically influences the flow turbulence, very few regions of high flow turbulence are observed for lower flow velocity, whereas a greater portion of highly disordered flow is noticed at 10 m/s velocity.

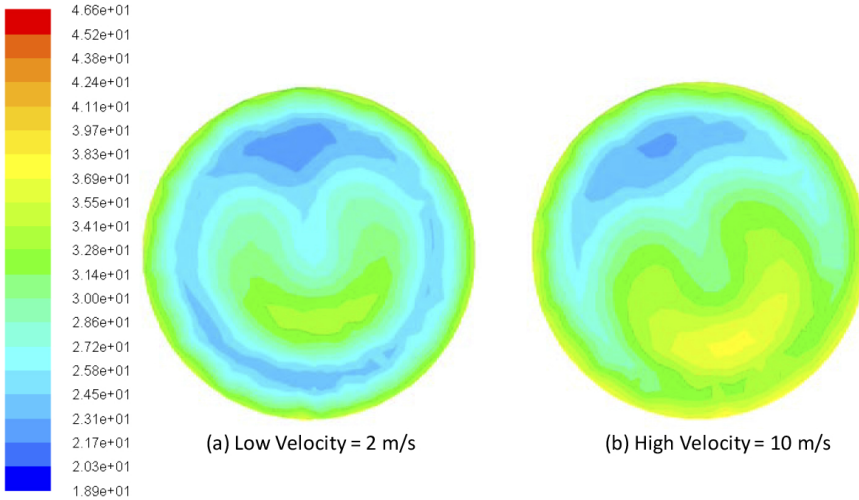

Fig. 12. Turbulent intensity at pipe outlet for 200 μm size particle

4.4. Pressure drop estimation

The pumping power of a slurry pump is significantly affected by the pressure head losses occurring during the slurry flow through the pipe. The high value of head losses in the pipe will lead to the requirement of higher pumping power to discharge the slurry at the same operating condition. Fig. 13 represents the variation in pressure drop calculated in the meter of water column with the flow velocity at a different solid concentration (5 to 20% by weight). It can be observed from the figure that the single-phase flow of water contributes to a negligible pressure drop

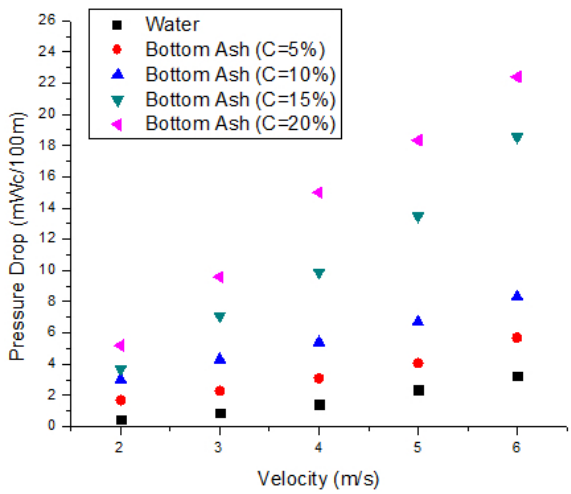

Fig. 13. Pressure head loss variation with flow velocity at different particulate concentration

at all velocity. However, increasing the particulate concentration will lead to much higher head loss. For instance, the slurry flow having 20% bottom ash by weight will create 2 times higher pressure reduction than that by 10% particulate slurry at the same velocity of 5 m/s. The trends are very similar to the findings in [25] with fly ash slurry.

4.5. Particle concentration effect

To analyze the effect of bottom ash concentration on the erosion wear, the operating conditions listed in test 5 to 7 of Table 3 are adopted. Fig. 14 shows the influence of bottom ash concentration on the erosion wear of the mild steel pipe. Enhancement in the magnitude of maximum erosion rate is observed as the concentration of the bottom ash in the slurry increases. The maximum erosion rate was enhanced to approximately 10 times when the contamination of bottom ash was increased from 2 to 10%. The increase in the concentration of the solid particle in the slurry will cause a larger number of solid particles to attack the wall which leads to high wear rate.

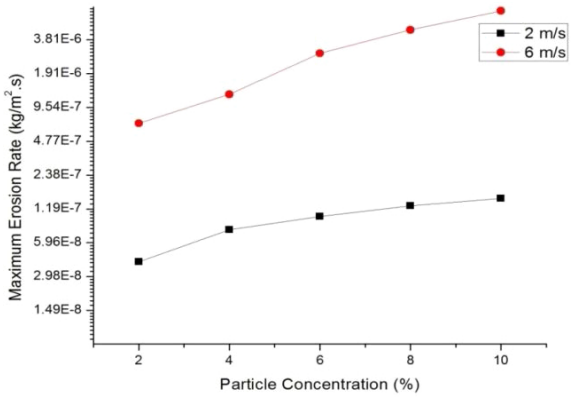

Fig. 14. Influence of particle contamination on erosion rate

5. Conclusions

A CFD-FLUENT-based model coupled with Discrete Phase Modeling scheme has been implemented to predict the erosion rate in the long straight pipe for the flow of bottom ash and water slurry. The influences of several parameters, like solid concentration, particle diameter and flow velocity on erosion rate were investigated. All the parameters were found to have a direct relationship with the erosion rate. The details of fluidic of multiphase regime inside the pipe is presented. Some of the important concluding remarks can be drawn from this work, such as:

- Larger sized particles possess high inertia and thus get deviated from the main fluid stream, hence more collision with the pipe wall is observed.

An enhancement of about 34% maximum erosion rate is noticed when the particle size increases from 250 to 300 μm.

- The erosion damage is mainly observed near the mid pipe length to the pipe exit.
- High particle settling is observed across the mid-length of the pipe, and it further increases up to the exit section.
- Pressure drop shares a direct relationship with particle concentration and flows velocity; the higher particulate concentration in the slurry will lead to much higher pressure drop and ultimately will reduce the pumping power.
- An increase in the percentage contamination of solid particle exerts a serve effect on the erosion characteristics. The maximum erosion rate was found to be to approximately 10 times of its initial magnitude when the contamination of bottom ash was increased from 2 to 10%.

Manuscript received by Editorial Board, March 24, 2018;
final version, June 28, 2018.

References

[1] C.A. Shook. Developments in hydrotransport. *The Candian Journal of Chemical Engineering*, 54(1-2):13–25, 1976. doi: 10.1002/cjce.5450540103.

[2] O.P. Modi, R. Dasgupta, B.K. Prasad, A.K. Jha, A.H. Yegneswaran, and G. Dixit. Erosion of a high-carbon steel in coal and bottom-ash slurries. *Journal of Materials Engineering and Performance*, 9(5):522–529, 2000. doi: 10.1361/105994900770345647.

[3] L. Zeng, G.A. Zhang, and X.P. Guo. Erosion–corrosion at different locations of X65 carbon steel elbow. *Corrosion Science*, 85:318–330, 2014. doi: 10.1016/j.corsci.2014.04.045.

[4] M.S. Patil, E.R. Deore, R.S. Jahagirdar, and S.V. Patil. Study of the Parameters Affecting Erosion Wear of Ductile Material in Solid-Liquid Mixture. In: *Proceedings of the World Congress of Engineering*, London, UK, 6–8 July, 2011.

[5] D.J. Bergstrom, T. Bender, G. Adamopoulos, and J. Postlethwaite. Numerical prediction of wall mass transfer rates in turbulent flow through a 90° two-dimensional bend. *The Canadian Journal of Chemical Engineering*, 76(2):728–737, 1998. doi: 10.1002/cjce.5450760407.

[6] C.A. Shook, M. McKibben, and M. Small. Experimental investigation of some hydrodynamic factors affecting slurry pipeline wall erosion. *The Canadian Journal of Chemical Engineering*, 68(1):17–23, 1990. doi: 10.1002/cjce.5450680102.

[7] S.K. Das. Mathematical model to predict effects of fly ash hardness and angularity on erosion response of typical boiler grade steels. *Tribology – Materials, Surfaces & Interfaces*, 6(2):84–92, 2012. doi: 10.1179/1751583112Z.00000000012.

[8] H.M. Badr, M.A. Habib, R. Ben-Mansour, and S.A.M. Said. Effect of flow velocity and particle size on erosion in a pipe with sudden contraction. The 6th Saudi Engineering Conference, vol.5:79–95, Dhahran, December 2002.

[9] E. Avcu, S. Fidan, Y. Yildiran, and T. Sinmazçelik. Solid particle erosion behaviour of Ti6Al4V alloy. *Tribology – Materials, Surfaces & Interfaces*, 7(4):201–210, 2013. doi: 10.1179/1751584X13Y.0000000043.

[10] V. Kannojiya, S. Kumar, M. Kanwar, and S.K. Mohapatra. Simulation of erosion wear in slurry pipe line using CFD. *Applied Mechanics and Materials*, 852:459–465, 2016. doi: 10.4028/www.scientific.net/AMM.852.459.

[11] M.A. Manzar and S.N. Shah. Particle distribution and erosion during the flow of Newtonian and non-Newtonian slurries in straight and coiled pipes. *Engineering Applications of Computational Fluid Mechanics*, 3(3):296–320, 2009. doi: 10.1080/19942060.2009.11015273.

[12] R. Zhang, H. Liu, and C. Zhao. A probability model for solid particle erosion in a straight pipe. *Wear*, 308(1–2):1–9, 2013. doi: 10.1016/j.wear.2013.09.011.

[13] B.S. McLaury, J. Wang, S.A. Shirazi, J.R. Shadley, and E.F. Rybicki. Solid particle erosion in long radius elbows and straight pipes. Annual Technical Conference and Exhibition, San Antonio, Texas, 5–8 October 1997. doi: 10.2118/38842-MS.

[14] A.M. Rashidi, M. Paknezhad M, M.R. Mohamadi-Ochmoushi and M. Moshrefi-Torbati. Comparison of erosion, corrosion and erosion-corrosion of carbon steel in fluid containing micro- and nanosize particles. *Tribology – Materials, Surfaces & Interfaces*, 7(3):114–121, 2013. doi: 10.1179/1751584X13Y.0000000039.

[15] V. Kannojiya, M. Deshwal, and D. Deshwal. Numerical analysis of solid particle erosion in pipe elbow. *Materials Today Proceedings*, 5(2):5021–5030, 2018. doi: 10.1016/j.matpr.2017.12.080.

[16] P. Goosen and I. Malgas. An experimental investigation into aspects of wear in boiler ash disposal pipelines. 14th International Conference on Slurry Handling and Pipeline Transport, Maastricht, The Netherlands, 8–10 September 1999.

[17] A.K. Ekambara, R.S. Sanders, K. Nandakumar, J.H. Masliyah. Hydrodynamic simulation of horizontal slurry pipeline flow using ANSYS-CFX. *Industrial and Engineering Chemistry Research*, 48(17):8159–8171, 2009. doi: 10.1021/ie801505z.

[18] J. Schaan, R. Sumner, R.G. Gillies, and C. Shook. The effect of particle shape on pipeline friction for Newtonian slurries of fine particles. *The Canadian Journal of Chemical Engineering*, 78(4):717–725, 2000. doi: 10.1002/cjce.5450780414.

[19] H. Wu, X. Liang, and Z. Deng. Numerical simulation on typical parts erosion of the oil pressure pipe line. *Thermal Science*, 17(5):1349–1353, 2013. doi: 10.2298/TSCI1305349W.

[20] M.R. Safaei, O. Mahian, F. Garoosi, K. Hooman, A. Karimipour, S.N. Kazi, and S. Gharehkhani. Investigation of micro- and nanosized particle erosion in a $90^{c}irc$ pipe bend using a two-phase discrete phase model. *The Scientific World Journal*, 2014. doi: 10.1155/2014/740578.

[21] S.A. Morsi and A.J. Alexander. An investigation of particle trajectories in two-phase flow systems. *Journal of Fluid Mechanics*, 55(2):193–208, 1972. doi: 10.1017/S0022112072001806.

[22] Fluent 2006 Fluent User's Guide.Lebanon, NH, Fluent Inc.

[23] M.K. Singh, S. Kumar, and D. Ratha. Computational analysis on disposal of coal slurry at high solid concentrations through slurry pipeline. *International Journal of Coal Preparation and Utilization*, 2017. doi: 10.1080/19392699.2017.1346632.

[24] W. Peng and X. Cao. Numerical simulation of solid particle erosion in pipe bends for liquid–solid flow. *Powder Technology*, 294:266–279, 2016. doi: 10.1016/j.powtec.2016.02.030.

[25] S. Chandel, V. Seshadri, and S.N. Singh. Effect of additive on pressure drop and rheological characteristics of fly ash slurry at high concentration. *Particulate Science and Technology*, 27(3): 271–284, 2009. doi: 10.1080/02726350902922036.